

# Geophysical Research Letters



## RESEARCH LETTER

10.1029/2020GL091384

### Key Points:

- Similarities and differences of magnetic conjugacy between Pc1 waves and isolated proton precipitation are reported
- The proton aurora shows a strong similarity with Pc1 waves in the same hemisphere, not characterized by classical cyclotron resonance
- This study suggests the importance of ionosphere for Pc1 waves by an ionospheric current modulation of an isolated proton aurora

### Supporting Information:

- Supporting Information S1
- Movie S1

### Correspondence to:

M. Ozaki,  
[ozaki@is.t.kanazawa-u.ac.jp](mailto:ozaki@is.t.kanazawa-u.ac.jp)









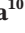






### Citation:

Ozaki, M., Shiokawa, K., Horne, R. B., Engebretson, M. J., Lessard, M., Ogawa, Y., et al. (2021). Magnetic conjugacy of Pc1 waves and isolated proton precipitation at subauroral latitudes: Importance of ionosphere as intensity modulation region. *Geophysical Research Letters*, 48, e2020GL091384. <https://doi.org/10.1029/2020GL091384>

Received 22 OCT 2020

Accepted 8 JAN 2021

## Magnetic Conjugacy of Pc1 Waves and Isolated Proton Precipitation at Subauroral Latitudes: Importance of Ionosphere as Intensity Modulation Region

Mitsunori Ozaki<sup>1</sup> , Kazuo Shiokawa<sup>2</sup> , Richard B. Horne<sup>3</sup> , Mark J. Engebretson<sup>4</sup> , Marc Lessard<sup>5</sup> , Yasunobu Ogawa<sup>6,7,8</sup> , Keisuke Hosokawa<sup>9</sup> , Masahito Nosé<sup>2</sup> , Yusuke Ebihara<sup>10</sup> , Akira Kadokura<sup>6,7,8</sup> , Satoshi Yagitani<sup>1</sup> , Yoshizumi Miyoshi<sup>2</sup> , Shion Hashimoto<sup>1</sup> , Shipra Sinha<sup>11</sup>, Ashwini K. Sinha<sup>11</sup>, Gopi K. Seemala<sup>11</sup> , and Chae-Woo Jun<sup>2</sup> 

<sup>1</sup>Graduate School of Natural Science and Technology, Kanazawa University, Kanazawa, Japan, <sup>2</sup>Institute for Space-Earth Environmental Research, Nagoya University, Nagoya, Japan, <sup>3</sup>British Antarctic Survey, Cambridge, UK, <sup>4</sup>Augsburg University, Minneapolis, MN, USA, <sup>5</sup>University of New Hampshire, Durham, NH, USA, <sup>6</sup>National Institute of Polar Research, Tachikawa, Japan, <sup>7</sup>Department of Polar Science, The Graduate University for Advanced Studies, SOKENDAI, Tachikawa, Japan, <sup>8</sup>Joint Support-Center for Data Science Research, Research Organization of Information and Systems, Tachikawa, Japan, <sup>9</sup>The University of Electro-Communications, Chofu, Japan, <sup>10</sup>Research Institute for Sustainable Humanosphere, Kyoto University, Uji, Japan, <sup>11</sup>Indian Institute of Geomagnetism, Navi Mumbai, India

**Abstract** Pc1 geomagnetic pulsations, equivalent to electromagnetic ion cyclotron waves in the magnetosphere, display a specific amplitude modulation, though the region of the modulation remains an open issue. To classify whether the amplitude modulation has a magnetospheric or ionospheric origin, an isolated proton aurora (IPA), which is a proxy of Pc1 wave-particle interactions, is compared with the associated Pc1 waves for a geomagnetic conjugate pair, Halley Research Base in Antarctica and Nain in Canada. The temporal variation of an IPA shows a higher correlation coefficient (0.88) with Pc1 waves in the same hemisphere than that in the opposite hemisphere. This conjugate observation reveals that the classic cyclotron resonance is insufficient to determine the amplitude modulation. We suggest that direct wave radiation from the ionospheric current by IPA should also contribute to the amplitude modulation.

**Plain Language Summary** The amplitude of electromagnetic ion cyclotron (EMIC) waves in the magnetosphere, which are observed as Pc1 waves on the ground, is an important parameter for characterizing the loss of energetic particles. The generation region of EMIC waves is well understood as being the magnetic equator, but the amplitude modulation region is not well-established due to wide horizontal Pc1 wave propagation in ionospheric ducts. Here we compare the properties of Pc1 waves and isolated proton precipitation from an ideal geomagnetic conjugate observation at Halley Research Base in Antarctica and Nain in Canada. By visualizing the cyclotron resonance region in the magnetosphere as an isolated proton aurora (IPA), the ambiguity of the horizontal propagation effects of Pc1 waves in the ionosphere is ideally removed. The observed IPA in the northern hemisphere has remarkable similarities with Pc1 waves in the same northern hemisphere, but not the southern hemisphere, providing evidence that the temporal variations of wave amplitude can be characterized by an ionospheric current induced in the IPA, and cannot be described only by a classical cyclotron resonance mechanism at the magnetic equator. Therefore, this study suggests that an IPA ionospheric current contributes to temporal modulations of Pc1 waves on the ground.

## 1. Introduction

Electromagnetic ion cyclotron (EMIC) waves, which are generated by sufficient temperature anisotropies in energetic ions (Anderson et al., 1992; Cornwall, 1965; Kennel & Petschek, 1966), have an important role in the loss of relativistic electrons in the radiation belts (Jordanova et al., 2008; Miyoshi et al., 2008; Ni et al., 2015; Omura & Zhao, 2013; Rodger et al., 2008; Shprits et al., 2017; Summers & Thorne, 2003) and of ring current ions into the atmosphere (Jordanova et al., 2001; Sakaguchi et al., 2015; Usanova et al., 2010; Yahnin et al., 2007; Zhou et al., 2019) through a wave-particle interaction regime. EMIC waves in the magnetosphere are equivalent to Pc1 (0.2–5 s) geomagnetic pulsations on the ground with no significant dif-

© 2021. The Authors.

This is an open access article under the terms of the [Creative Commons Attribution-NonCommercial-NoDerivs License](https://creativecommons.org/licenses/by-nc-nd/4.0/), which permits use and distribution in any medium, provided the original work is properly cited, the use is non-commercial and no modifications or adaptations are made.

ference in frequency dispersion between satellite and ground observations (e.g., Paulson et al., 2014). Both EMIC and Pc1 waves show various temporal characteristics of amplitude modulations known as pearl structures constructing a one wave packet (several tens of seconds to a few minutes; Saito, 1969; Troitskaya & Gul'Elmi, 1967), subpacket structures contained within a wave packet (a few tens of seconds; Nakamura et al., 2015), and generation frequency. Previous studies have all reported isolated proton aurora (IPA) events including the temporal characteristics of Pc1 waves at subauroral latitudes (intervals between neighbor wave packets, Nomura et al., 2016; subpacket structures, Ozaki et al., 2016; Pc1 frequency range, Ozaki et al., 2018). This direct link between Pc1 waves and IPAs suggests that the seed region of precipitating particles for IPA is the magnetic equator (Sakaguchi et al., 2015; Yahnin et al., 2007), but the specific location for the wave amplitude modulation is still an open issue. In this study, we focus on the modulation region for pearl structures showing a larger amplitude variation. Understanding the origin of the amplitude modulation region of EMIC/Pc1 waves is important for better quantitative models of global flux and energy in the radiation belts and space weather forecasting because the precipitating flux is characterized by the wave amplitude at the wave-particle interaction region (Albert & Bortnik, 2009; Summers & Thorne, 2003). Currently, amplitude modulation models of EMIC/Pc1 waves are mainly classified into two categories. In the first category, the amplitude modulation is generated at the equatorial source region in the magnetosphere (e.g., modulation of the wave growth rate by ULF waves, Loto'aniu et al., 2009). In the second category there are no associated wave-particle interactions in the magnetosphere (e.g., the effects of bouncing wave propagation between the northern and southern hemispheres (Obayashi, 1965) and the beat effects in the ionosphere by the superposition of Pc1 waves (Nomura et al., 2011; Jun et al., 2014; 2016)). Since Pc1 waves can horizontally propagate over several thousands of km in ionospheric ducts (Fujita & Tamao, 1988; H. Kim et al., 2010), it is difficult to identify whether or not the modulation region is generated in the magnetosphere, even by geomagnetic conjugate observations of Pc1 waves in both hemispheres. For this reason, IPAs are a useful indicator of wave-particle interaction regions for determining the horizontal propagation effects of Pc1 waves in the ionosphere. However, simultaneous measurements of IPAs and conjugate Pc1 waves have not yet been performed.

Here, we present a case study of conjugate observations of Pc1 waves on the ground in combination with precipitating particles into the atmosphere at geomagnetic conjugate sites: Halley Research Station in Antarctica (Geomagnetic 67.4°S, 27.7°E) and Nain in Canada (Geomagnetic 66.3°N, 14.5°E) in subauroral latitudes. If the modulation region of wave amplitude corresponds with the wave-particle interaction region in the magnetosphere, the intensity variation of the northern IPA will be correlated with that of the southern Pc1 waves because of the cyclotron resonance between EMIC waves and counter-streaming energetic protons at the magnetic equator. In contrast to typical cyclotron resonance, the intensity variation of the northern IPA observed in this case study is similar to that of the northern Pc1 waves, suggesting that the modulation region is localized in the ionosphere. For an ionospheric origin, the Pc1 waves must exhibit not only the effects of wave-particle interactions in the magnetosphere for the seed particle population but also additional modulation processes in the ionosphere. This study will help in understanding cyclotron resonance in the magnetosphere and any further processes in the ionosphere for coupling between Pc1 waves and IPA.

## 2. Wave, Aurora, and Particle Data

### 2.1. Ground-Based Magnetometers

We focus primarily on ground-based magnetometer data at Halley and Nain. At Halley, run by the British Antarctic Survey (BAS), an induction magnetometer is operated with a sampling frequency of 10 Hz. The magnetometer data at Halley are collected far from artificial facilities and hence contain no contamination by artificial electromagnetic noise. At Nain, an observation site of the Magnetometer Array for Cusp and Cleft Studies (MACCS), fluxgate magnetometer data is recorded with a 0.5-s resolution (Engebretson et al., 1995). The spectrum subtraction method (Boll, 1979), which is a general technique in noise suppression, is applied to the Nain data, because the data include some noise. There is no specific difference in the temporal variations of Pc1 waves measured at Nain before and after the noise suppression (see Figure S1 in Supporting Information (SI)).

## 2.2. Auroral Images

We used all-sky images obtained by the Time History of Events and Macroscale Interactions during Substorms (THEMIS) all-sky imager (ASI) at Goose Bay (GBAY, Geographic 53.3°N, 60.4°W) near Nain (S. B. Mende et al., 2008). The all-sky image is panchromatic with a temporal resolution of 3 s. For a global image, we used data from the Special Sensor Ultraviolet Spectrographic Imager (SSUSI) on board the Defense Meteorological Satellite Program (DMSP) F18 satellite (Paxton et al., 2002). Specifically, we used the Lyman  $\alpha$  (121.6 nm) channel for identifying proton precipitation and the N2 Lyman-Birge-Hopfield long (LBHL, 160–180 nm) channel for energetic particle precipitation (Immel et al., 2002). The DMSP satellite orbiting at an altitude of  $\sim$ 850 km provides a wide spatial coverage using a weather-impervious imager, and the use of a ground-based imager at a fixed location gives a high temporal resolution.

## 2.3. Proton Precipitation by Satellites

To confirm the precipitation of energetic protons into the ionosphere, we used data from the Medium Energy Proton and Electron Detector (MEPED) instrument at the Polar Operational Environmental Satellite (POES; Evans & Greer, 2000) and the Meteorological Operational (MetOp) satellite formation. The MEPED instrument has several energy channels for protons, but we used the 80–250 keV channel data as a typical proxy of an IPA (Miyoshi et al., 2008; Yahnin et al., 2007).

## 3. Conjugate Observation Event

Figure 1 shows a notable case of conjugate Pc1 waves in the typical He<sup>+</sup> band (see Text S1 in SI) and a related IPA during 00:30–3:30 UT (post-midnight zone in MLT) on February 7, 2011 in a late recovery phase of a magnetic storm (Dst index:  $-28$  to  $-25$  nT). The dynamic spectrum of Pc1 waves ( $\sqrt{B_x^2 + B_y^2}$ ) in Halley (Figure 1c) looks similar to that for Nain (Figure 1e), but the wave intensity for Halley is approximately five-times larger than that for Nain, where  $B_x$  and  $B_y$  are north to south and east to west components, respectively. The wave transmission in the ionosphere depends on the source location and the electron density (Fedorov et al., 2018). The detailed spatial distribution of the source region is shown later in Figure 2, the dominant factor of the wave attenuation can be the difference in the electron density. The electron density in the E region above Halley is 10-times higher than that for Nain from the international reference ionosphere model (Bilitza, 2018) because Halley is under the condition of sunshine. The wave intensity in the ionosphere above Halley can be over five-times stronger than that of Nain. The Pc1 waves show typical rising tone structures. The frequency sweep rate is approximately 260 s/Hz and becomes gradually larger up to 1,080 s/Hz with time. On the other hand, the polarization profiles of Pc1 waves at both sites do not show a high similarity. The polarization at Halley (Figure 1d) first shows a right-handed polarization for the whole frequency range, then changes to left-handed and right-handed polarizations, and finally taking different properties in each frequency range. The polarization at Nain (Figure 1f) shows a pure right-handed polarization over the whole frequency range. In this event, a related IPA is observed at GBAY (Figures 1b and 1g; see Video S1 in SI). A weak IPA arc gradually moves equatorward from the northward edge in the field of view from 00:30 UT (in Figure 1g, the initial auroral arc is not clear before 01:35 UT, but it is clearly seen in Video S1). Then, the IPA intensity is significantly enhanced at 01:35 UT. The enhanced IPA intensity becomes weak from 02:30 to 02:40 UT, but the IPA intensity increases again from 02:40 UT, and the IPA was finally blinded at 03:20 UT. This temporal agreement supports the observed IPA being a signature of the location of the wave-particle interaction region in the magnetosphere for the Pc1 waves. In particular, the IPA moves to the lower-latitude side as the lower limit frequency of the Pc1 waves increases. Although each of the Pc1 waves at Halley and Nain widely propagates in the ionospheric duct in both hemispheres (see Figure S2 in SI), this conjugate observation of Pc1 waves at Halley and Nain suggests that the horizontal propagation effects in the ionospheric duct should be ignored because of the very close positional relation with the IPA.

This study has an advantage of visualizing the spatial scale of the source size. Figure 2a shows the northern global auroral image at a wavelength of 121.6 nm measured by the SSUSI/DMSP F18 satellite and a snapshot of the IPA at GBAY taken on 01:40 UT passing above GBAY on the geomagnetic map in dipole



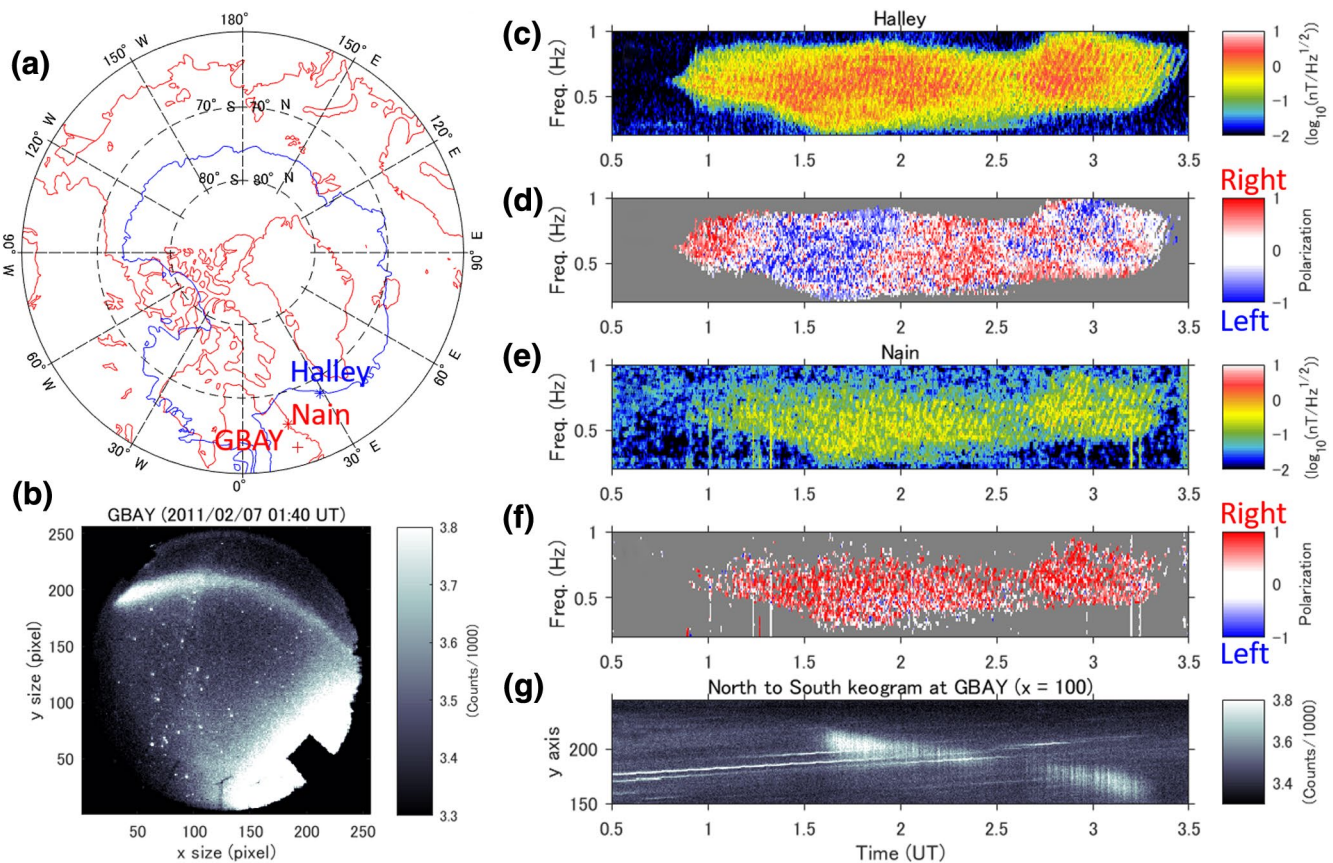


**Figure 1.** Geomagnetic conjugate observation of Pc1 waves and an IPA on February 7, 2011. (a) Halley, Nain, and GBAY on the geomagnetic map. The blue and red lines indicate coastlines for the southern and northern hemispheres, respectively. ((b) and (g)) All-sky image and keogram of the IPA at GBAY. ((c) and (d)) Dynamic spectrum and polarization of Pc1 waves at Halley. (e and f) Dynamic spectrum and polarization of Pc1 waves at Nain. IPA, isolated proton aurora; GBAY, Goose Bay.

coordinates using the coefficients from the International Geomagnetic Reference Field 2011 model (Finlay, 2010). The images are projected assuming an auroral altitude of 110 km. The IPA observed by the THEMIS ASI is connected with the same location of isolated emission at 121.6 nm, which strongly supports that this auroral event is excited by the precipitating energetic protons. The IPA was not observed eastward of 30° by the THEMIS-ASI at Narsarsuaq, Greenland (Geographic 61.2°N, 45.4°E). The IPA is spread over a very narrow latitude range within a 1-deg width, but over a wide longitudinal range within 30-deg width. Figure 2b shows the southern global image of N2 LBHL (160.0–180.0 nm) band emissions by the SSUSI/DMSF F18 satellite and precipitating 80–250 keV protons by the POES and MetOp satellites. The auroral oval boundary is seen around the magnetic latitude of 75° from the LHBL emissions, but the related proton precipitation is seen at lower latitudes of ~66°. The POES and MetOp satellites detected isolated proton precipitation near latitudes of the northern IPA, which supports not only conjugate Pc1 waves but also conjugate proton precipitation in both hemispheres (Zhang & Paxton, 2019).

#### 4. Similarities and Differences in Magnetic Conjugacy

In order to distinguish the magnetospheric origin of the Pc1 intensity modulation, we evaluated the similarities and differences between the characteristics of the northern IPA and Pc1 waves in both hemispheres. Since the durations of the IPA and Pc1 waves were much longer than the time taken for the orbiting satellites to pass a fixed ground location, ground-based observations allowed an ideal comparison between the IPA and Pc1 waves to be made.

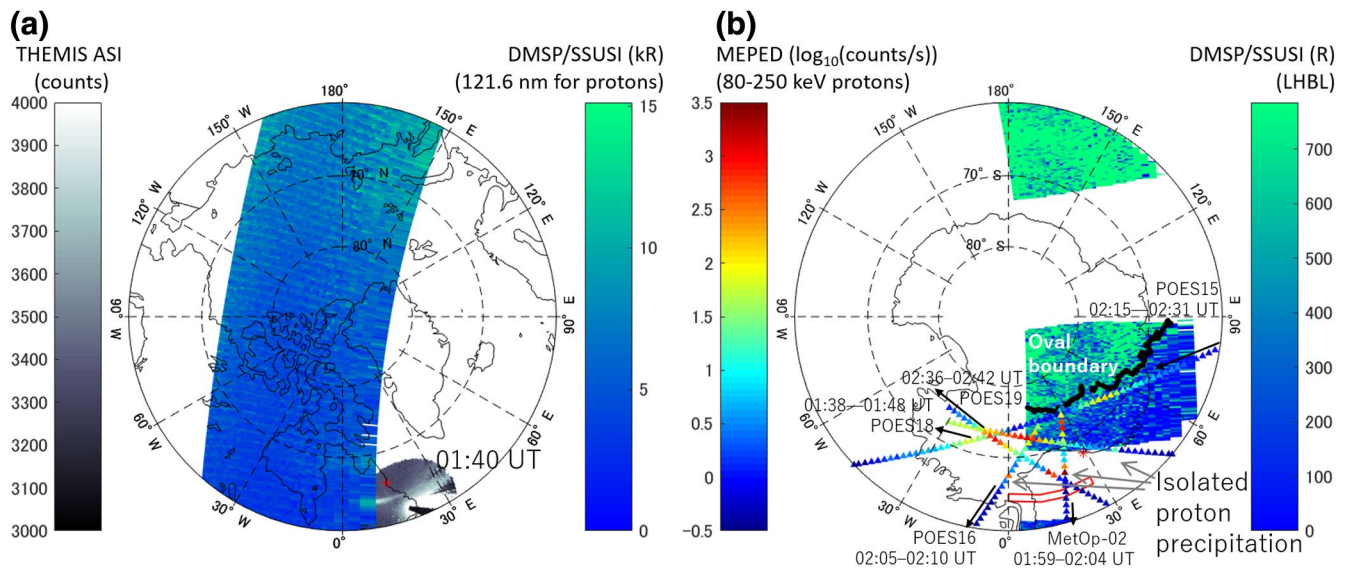


**Figure 2.** Global images of isolated proton precipitation at (a) the northern (averaged UT 01:48) and (b) southern (averaged UT 00:54) hemispheres. The red square indicates the location of the northern IPA. The Nain and Halley locations are indicated by asterisks. The global image in the southern hemisphere is partially masked by an error flag. The black solid line indicates the equatorward boundary of auroral oval in the southern hemisphere. The triangle symbols indicate the precipitation of 80–250 keV protons observed by POES and MetOp satellites at the ionospheric footprints. IPA, isolated proton aurora; POES, Polar Operational Environmental Satellite; MetOp, Meteorological Operational.

The IPA includes luminous modulations with a time scale similar to that of the Pc1 rising-tone elements. The dominant periodicity of the Pc1 intensity variation at Halley was 7.18 mHz (see Figure S3a and Text S2 in SI), which is equivalent to the interval between the rising tone elements. The dominant periodicities of the Pc1 intensity variation at Nain were 6.24 and 6.92 mHz (see Figure S3b in SI). The periodicity of the Pc1 waves in both hemispheres shows similar values in the range from 6.24 to 6.67 mHz, but a different shorter periodicity (7.18–7.61 mHz) at Halley was dominant. The spatial distribution of the periodicity in the IPA is shown in Figure S4 in SI. The periodicity of the northern IPA intensity variation was 6.75 mHz, similar to the periodicity of Pc1 waves at Nain but not at Halley (See Figure S3c in SI).

The measurement of isolated proton precipitation by the satellites passing the southern hemisphere shows that the latitude range is less than 1°, and similarly for the northern IPA, but the longitude range can be over 30°. This difference in the longitudinal width in both hemispheres can be due to the different widths of the equatorial loss cone in each hemisphere. In this event, the loss cone width for south-going particles was 3.67°, while the loss cone for north-going particles was a smaller value of 3.58° from the Tsyganenko, 2002a, 2002b model (Tsyganenko, 2002a, 2002b) because of the effects of the South Atlantic Magnetic Anomaly (SAMA; Selesnick et al., 2003).

Next, we calculated the cross correlation values between the northern IPA and Pc1 waves in both hemispheres with a temporal resolution of 9 s. The wave propagation time and traveling time of precipitating protons from the equator are several tens of seconds, so a 9-s temporal resolution is sufficient to classify the origin as being magnetosphere or ionosphere. The first point to note is that the Pc1 waves arrived at Halley approximately 117 s earlier than at Nain (see Figure S5 in SI). The cross wavelet analysis between the Halley and Nain Pc1 wave intensities is shown in Figure S6 in SI, but the bouncing of each wave packet was not clear because of the dense overlapping of wave elements. Second, the maximum correlation between the northern IPA and Pc1 intensity at Halley (Figure 3a) was 0.79 without a clear peak, and the time difference between them was widely distributed in a 99% range from –1,503 to +1,557 s (gray area) from the maximum correlation at –18 s shown in Figure 3b. Third, the correlation between the northern IPA and Pc1 intensity at Nain (Figure 3c) shows a clear peak (0.88) with almost no time difference between them (less than the time resolution of 9 s; see Figures 3d and S7 in SI). Notably, enhancement of intensity variations of Pc1 waves from 03:00 to 03:20 UT is only seen in the Pc1 waves at Nain along with an associated enhancement of IPA intensity variation. These relationships are the same in all cases using intensity variations calculated by

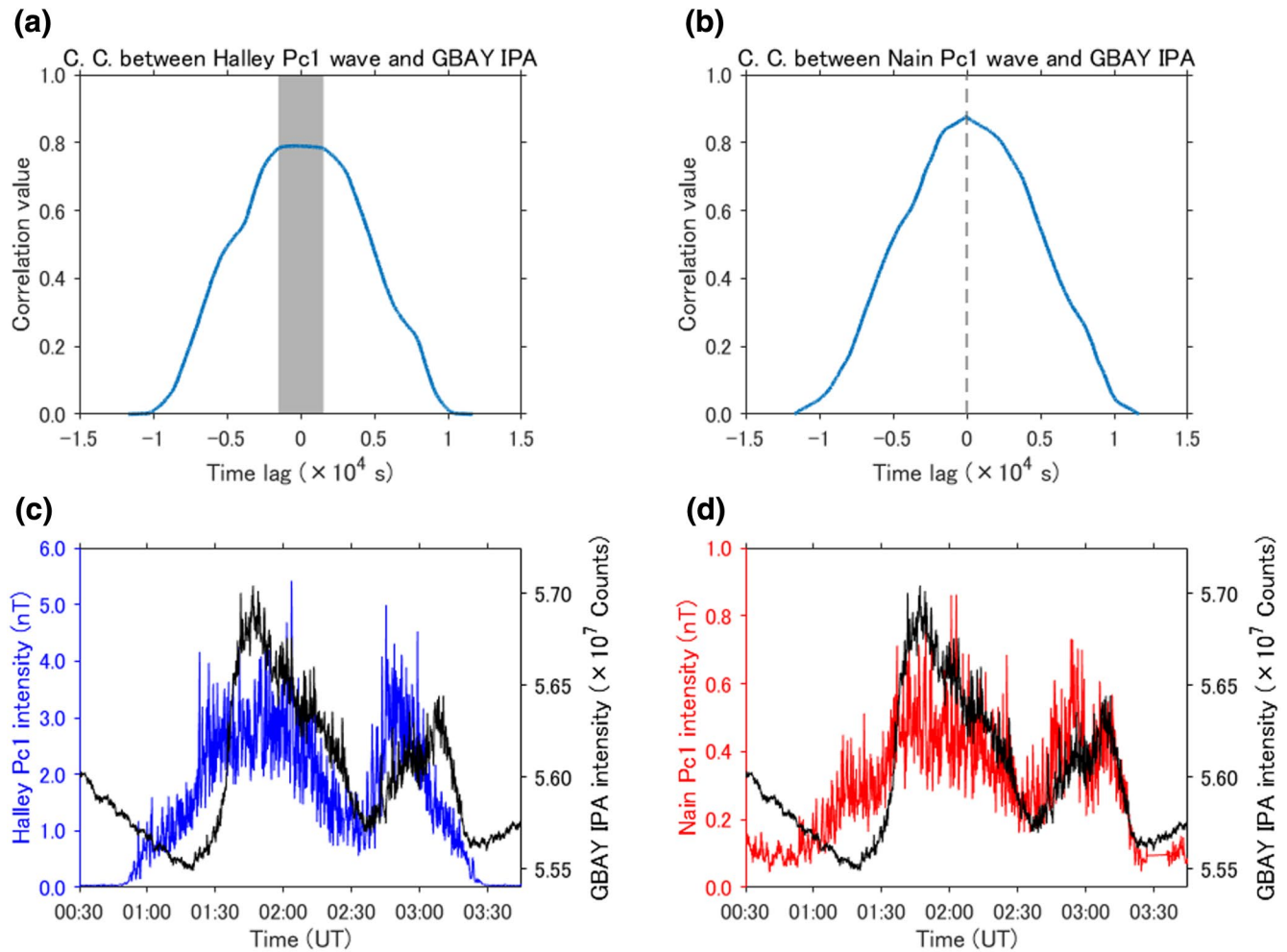


**Figure 3.** Cross-correlation analysis between northern IPA and Pc1 waves at both hemispheres. (a) and (b) Correlation between Halley Pc1 and GBAY IPA and their intensity variations. The GBAY IPA intensity variation is plotted with a  $-18$ -s time lag given the maximum correlation value. (c) and (d) Correlation between Nain Pc1 and GBAY IPA and their intensity variations with almost no time lag. The positive value of time lag means Pc1 waves arrived at the observation site later than the IPA. GBAY, Goose Bay; IPA, isolated proton aurora.

other methods (with a different overlap, time resolution, and frequency resolution for FFT). From a simple calculation model based on S. Mende et al. (1980) and Ozaki et al. (2018), the time difference of 117 s between the Halley Pc1 and GBAY IPA was not consistent with the modulation mechanism near the equator, for direct traveling and reflected traveling at the opposite hemisphere and the predicted time difference of 40 s due to the long time lag. Therefore, the observed higher similarity between GBAY IPA and Nain Pc1 waves suggests the existence of a common modulation mechanism for the Pc1 wave intensity and proton precipitation flux at the ionosphere in the same hemisphere.

## 5. Discussion and Conclusions

A conjugate event of Pc1 waves together with an IPA was successfully obtained from approximately 350 conjugate experiments at both hemispheres in the operation period from 2011 to 2015. Various conditions created difficulties in identifying the amplitude modulation region, namely geomagnetic activity, weather, geographical conditions, data archiving, and satellite orbiting issues. However, this well-coordinated conjugate observation enabled the similarities between the temporal variations of the IPA and Pc1 waves to be determined. The possibility of beat effects in the ionosphere by the superposition of Pc1 waves, which is considered to be a possible ionospheric origin for the amplitude modulation of Pc1 waves, was dismissed because it cannot explain the flux modulation of proton precipitation. Another possibility is the occurrence of



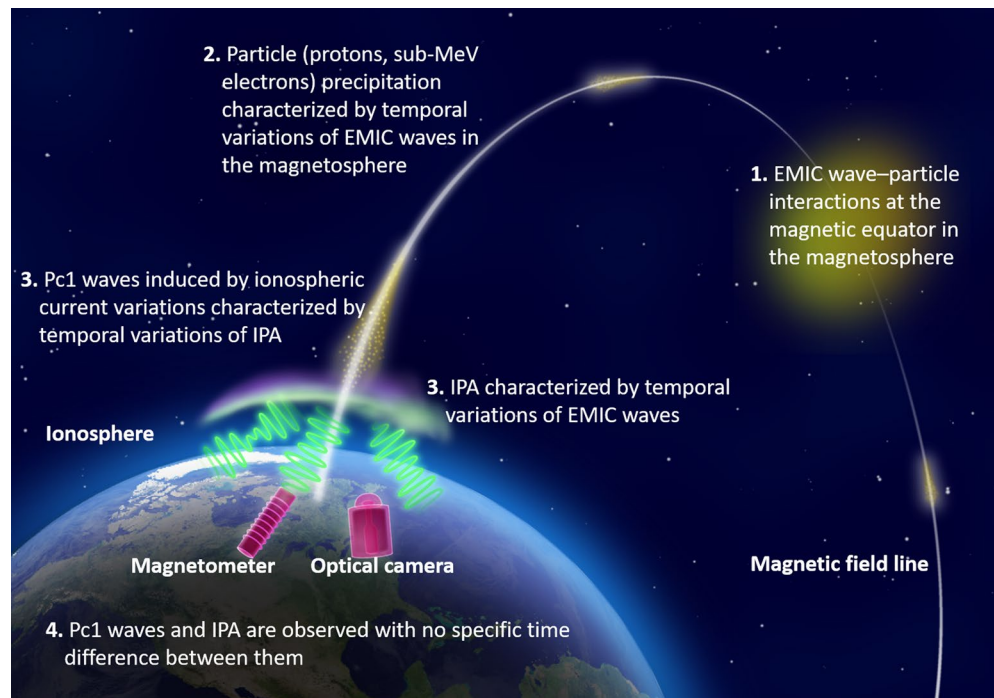


**Figure 4.** Schematic illustration of a possible scenario of Pc1 waves radiated from an IPA. IPA, isolated proton aurora.

similar effects for electron acceleration in the ionospheric Alfvén resonator (IAR) (Chaston et al., 2002), but harmonic structures as a signature of IAR at Nain could not be identified in the frequency range less than 1 Hz. At Halley, no IAR was observed. The observed modulations of the isolated auroral event thus are not due to electron acceleration from the effects of IAR. Although Pc1 waves on the ground can be equivalent to EMIC waves in the magnetosphere by mode conversion (left hand to right hand) or tunneling effects as major mechanisms (e.g., Paulson et al., 2017), the minimal observed time difference between the IPA and Pc1 waves at the same hemisphere precludes propagation from the magnetosphere.

Here, we consider two possibilities in which the ionosphere plays an important role in explaining the observations. One is a kind of duct effect along the field line. The particle precipitation can modulate the ionospheric currents and the conductivity and create additional ionization in the ionosphere, which together would enable the Pc1 waves to reach the ground more easily. This possibility of the IPA acting as a duct does not explain the observed high similarity between the temporal variations of the IPA and Pc1 waves at the same hemisphere. However, direct wave radiation from the IPA is possible, as in the same behavior that PiC geomagnetic pulsations accompanying ionospheric currents by pulsating auroras (Oguti, 1986). If an ionospheric current in the IPA can radiate Pc1 waves, the observed similarity between the northern IPA and Pc1 waves at Nain is more reasonably explicable (see Figure 4). EMIC waves in the magnetosphere can easily deviate from the magnetic field line connected to the wave-particle interactions (e.g., E. H. Kim & Johnson, 2016; Miyoshi et al., 2019). Then, the EMIC waves do not always have to penetrate the ionosphere in this scenario.

The ionospheric current due to an IPA can be slowed by the effects of recombination processes in the ionosphere. The time constant for an electron density to decay to the background level is typically 5–10 s in the E and D regions for pulsating auroras (Hosokawa et al., 2010) and precipitation electrons from the radiation belts (Lanzerotti & Rosenberg, 1983). This time constant is inversely proportional to the electron density and the recombination coefficients characterized by the temperature. Thus, at a lower temperature the electron density would be a few times higher and the recombination coefficients can be larger, which can lead to the direct radiation of Pc1 waves from the ionosphere with a shorter time constant of a few seconds (e.g., see Figure 3 in Semeter & Kamalabadi, 2005). In strong support of direct wave emission from an IPA, previous studies (Heacock & Hunsucker, 1977; Ozaki et al., 2018; Roldugin et al., 2013) showed that Pc1–2

geomagnetic pulsations are accompanied by auroral particle precipitation with the same Pc1–2 periods. Our results suggest that direct radiation of Pc1 waves from an IPA play a role in a modulation process localized in the ionosphere.

Let us summarize this case study of a remarkable conjugate event of Pc1 waves and isolated proton precipitation as follows:

- The dynamic spectra of Pc1 waves for Halley and Nain are similar, but the detailed properties (intensity, polarization, and periodicity) are different
- The narrow latitudinal widths of isolated proton precipitation in both hemispheres are similar, but the longitudinal range ( $>30^\circ$ ) in the southern hemisphere is wider than that in the northern hemisphere probably due to the effects of SAMA
- The temporal variations of the northern IPA are more similar to the northern Pc1 waves than the southern Pc1 waves. This supports the modulation region for wave amplitude being far from the wave-particle interaction region at the magnetic equator
- An ionospheric current induced in the enhancement of an IPA is a possible generation source for the amplitude modulation of Pc1 waves on the ground

The different properties of Pc1 waves on the ground at both hemispheres indicate that the modulation mechanisms can operate independently in the northern and southern hemispheres. Paulson et al. (2014, 2017) also reported from in-situ observations of Pc1 pearl structures that the bouncing wave packet model is not enough for determining the wave characteristics of Pc1 pearl pulsations. The present study indicates the importance of the difference of the ionospheres in the two hemispheres as an additional aspect of the process. We suggest that the wave properties in both hemispheres depend on the seasonal effects of the ionosphere, which will be confirmed by future studies. Finally, some wave and optical instruments were installed at Nain by the PWING (study of dynamical variation of Particles and Waves in the INner magnetosphere using Ground-based network observations) project (Shiokawa et al., 2017), and low-cost optical cameras for multi-wavelengths are planned to be installed at Halley (Ogawa et al., 2020). Future comprehensive conjugate observations of waves and optics at Halley and Nain will help to develop a new diagnostic approach for severe space weather by visualizing never-before-seen states of the modulation processes in the ionosphere at subauroral latitudes.

### Data Availability Statement

The authors wish to thank the BAS team for the continuous operation of the induction magnetometer at Halley (the data from <http://psddb.nerc-bas.ac.uk/data/access/download.php?menu=1&bc=1,4,7,8,9&source=1&class=101&type=SCM&site=Halley&year=2011&day=038&month=02&v=ascii>), the MACCS team for supplying magnetometer data at Nain (available from <http://space.augsburg.edu/maccs/retriev-eiaga2002.jsp?stations=NA&startYear=2011&month=1&dayOfMonth=7&startDay=38&GetData=Get+Data>), Johns Hopkins University Applied Physics Laboratory for providing the DMSP/SSUSI data (from [https://ssusi.jhuapl.edu/data\\_retriver?spc=f18&type=sdr&year=2011&Doy=038](https://ssusi.jhuapl.edu/data_retriver?spc=f18&type=sdr&year=2011&Doy=038)), and NOAA for supporting the MEPED data (from <https://satdat.ngdc.noaa.gov/sem/poes/data/processed/swpc/uncorrected/avg/cdf/2011/>). THEMIS-ASI data at GBAY are available from the THEMIS Science webpage (<http://themis.ssl.berkeley.edu/data/themis/thg/l1/asi/gbay/2011/02/>). The Dst index data were obtained from the World Data Center for Geomagnetism, Kyoto ([http://wdc.kugi.kyoto-u.ac.jp/dst\\_final/201102/index.html](http://wdc.kugi.kyoto-u.ac.jp/dst_final/201102/index.html)). The geomagnetic maps are drawn using the mapping package M\_Map (from <https://www.eoas.ubc.ca/~rich/map.html>).

### References

- Albert, J. M., & Bortnik, J. (2009). Nonlinear interaction of radiation belt electrons with electromagnetic ion cyclotron waves. *Geophysical Research Letters*, 36(12), L12110. <https://doi.org/10.1029/2009GL038904>
- Anderson, B. J., Erlanson, R. E., & Zanetti, L. J. (1992). A statistical study of Pc 1–2 magnetic pulsations in the equatorial magnetosphere: 2. Wave properties. *Journal of Geophysical Research*, 97(A3), 3089–3101. <https://doi.org/10.1029/91JA02697>
- Bilitza, D. (2018). IRI the international standard for the ionosphere. *Advances in Radio Science*, 16, 1–11. <https://doi.org/10.5194/ars-16-1-2018>

### Acknowledgments

This work was supported by JSPS KAKENHI Grant Numbers JP15H05815, JP16H06286, JP17K06456, JP20H01959, and JP20H02162 and by the research grant on Sustainable Humanosphere Science from the Research Institute for Sustainable Humanosphere (RISH), Kyoto University. R. B. Horne was supported in the UK by NERC National Capability grants NE/R016038/1 and NE/R016445/1. MACCS is operated by Augsburg University and funded by the U.S. National Science Foundation grant AGS-1651263. Support for this work was provided at UNH by NSF award ANT-1745041.



- Boll, S. (1979). Suppression of acoustic noise in speech using spectral subtraction. *IEEE Transactions on Acoustics, Speech, & Signal Processing*, 27(2), 113–120. <https://doi.org/10.1109/TASSP.1979.1163209>
- Chaston, C. C., Bonnell, J. W., Carlson, C. W., Berthomier, M., Peticolas, L. M., Roth, I., et al. (2002). Electron acceleration in the ionospheric Alfvén resonator. *Journal of Geophysical Research*, 107(A11), SMP41-1–SMP41-16. <https://doi.org/10.1029/2002JA009272>
- Cornwall, J. M. (1965). Cyclotron instabilities and electromagnetic emission in the ultra low frequency and very low frequency ranges. *Journal of Geophysical Research*, 70(1), 61–69. <https://doi.org/10.1029/JZ070i001p00061>
- Engebretson, M. J., Hughes, W. J., Alford, J. L., Zesta, E., Cahill, L. J., Arnoldy, R. L., & Reeves, G. D. (1995). Magnetometer array for cusp and cleft studies observations of the spatial extent of broadband ULF magnetic pulsations at cusp/cleft latitudes. *Journal of Geophysical Research*, 100(A10), 19371–19386. <https://doi.org/10.1029/95JA00768>
- Evans, D. S., & Greer, M. S. (2000). *Polar orbiting environmental satellite space environment monitor: 2. Instrument description and archive data documentation*. Boulder, CO: Tech. Memo. OAR SEC-93, NOAA.
- Fedorov, E. N., Pilipenko, V. A., Engebretson, M. J., & Hartinger, M. D. (2018). Transmission of a magnetospheric Pc1 wave beam through the ionosphere to the ground. *Journal of Geophysical Research: Space Physics*, 123(5), 3965–3982. <https://doi.org/10.1029/2018JA025338>
- Finlay, C. (2010). International geomagnetic reference field: The eleventh generation. International Association of Geomagnetism and Aeronomy, Working Group V-MOD, *Geophysical Journal International*, 183(3), 1216–1230. <https://doi.org/10.1111/j.1365-246X.2010.04804.x>
- Fujita, S., & Tamao, T. (1988). Duct propagation of hydromagnetic waves in the upper ionosphere, 1, Electromagnetic field disturbances in high latitudes associated with localized incidence of a shear Alfvén wave. *Journal of Geophysical Research*, 93(A12), 14665–14673. <https://doi.org/10.1029/JA093iA12p14674>
- Heacock, R. R., & Hunsucker, R. D. (1977). A study of concurrent magnetic field and particle precipitation pulsations, 0.005 to 0.5 Hz, recorded near College, Alaska. *Journal of Atmospheric and Terrestrial Physics*, 39(4), 487–501. [https://doi.org/10.1016/0021-9169\(77\)90158-1](https://doi.org/10.1016/0021-9169(77)90158-1)
- Hosokawa, K., Ogawa, Y., Kadokura, A., Miyaoka, H., & Sato, N. (2010). Modulation of ionospheric conductance and electric field associated with pulsating aurora. *Journal of Geophysical Research*, 115(A3), A03201. <https://doi.org/10.1029/2009JA014683>
- Immel, T. J., Mende, S. B., Frey, H. U., Peticolas, L. M., Carlson, C. W., Gerard, J.-C., et al. (2002). Precipitation of auroral protons in detached arcs. *Geophysical Research Letters*, 29(11), 141–144. <https://doi.org/10.1029/2001GL013847>
- Jordanova, V. K., Albert, J., & Miyoshi, Y. (2008). Relativistic electron precipitation by EMIC waves from self-consistent global simulations. *Journal of Geophysical Research*, 113(A3), A00A10. <https://doi.org/10.1029/2008JA013239>
- Jordanova, V. K., Farrugia, C. J., Thorne, R. M., Khazanov, G. V., Reeves, G. D., & Thomsen, M. F. (2001). Modeling ring current proton precipitation by electromagnetic ion cyclotron waves during the May 14–16, 1997, storm. *Journal of Geophysical Research*, 106(A1), 7–22. <https://doi.org/10.1029/2000JA002008>
- Jun, C.-W., Shiokawa, K., Connors, M., Schofield, I., Poddelsky, I., & Shevtsov, B. (2014). Study of Pc1 pearl structures observed at multi-point ground stations in Russia, Japan, and Canada. *Earth Planets and Space*, 66(140). <https://doi.org/10.1186/s40623-014-0140-8>
- Jun, C.-W., Shiokawa, K., Connors, M., Schofield, I., Poddelsky, I., & Shevtsov, B. (2016). Possible generation mechanisms for Pc1 pearl structures in the ionosphere based on 6 years of ground observations in Canada, Russia, and Japan. *Journal of Geophysical Research: Space Physics*, 121(5), 4409–4424. <https://doi.org/10.1002/2015JA022123>
- Kennel, C. F., & Petschek, H. E. (1966). Limit on stably trapped particle fluxes. *Journal of Geophysical Research*, 71(1), 1–28. <https://doi.org/10.1029/JZ071i001p00001>
- Kim, E.-H., & Johnson, J. R. (2016). Full-wave modeling of EMIC waves near the He<sup>+</sup> gyrofrequency. *Geophysical Research Letters*, 43(1), 13–21. <https://doi.org/10.1002/2015GL066978>
- Kim, H., Lessard, M. R., Engebretson, M. J., & Lühr, H. (2010). Ducting characteristics of Pc 1 waves at high latitudes on the ground and in space. *Journal of Geophysical Research*, 115(A9), A09310. <https://doi.org/10.1029/2010JA015323>
- Lanzerotti, L. J., & Rosenberg, T. J. (1983). Impulsive particle precipitation and concurrent magnetic field changes observed in conjugate areas near L = 4. *Journal of Geophysical Research*, 88(A11), 9115–9124. <https://doi.org/10.1029/JA088iA11p09115>
- Loto'aniu, T. M., Fraser, B. J., & Waters, C. L. (2009). The modulation of electromagnetic ion cyclotron waves by Pc5 ULF waves. *Annals of Geophysics*, 27(1), 121–130. <https://doi.org/10.5194/angeo-27-121-2009>
- Mende, S., Arnoldy, R., Cahill, L., Doolittle, J., Armstrong, W., & Fraser-Smith, A. (1980). Correlation between  $\lambda$ 4278-Å Optical emissions and a Pc 1 Pearl Event observed at Siple Station, Antarctica. *Journal of Geophysical Research*, 85(A3), 1194–1202. <https://doi.org/10.1029/JA085iA03p01194>
- Mende, S. B., Harris, S. E., Frey, H. U., Angelopoulos, V., Russell, C. T., Donovan, E., et al. (2008). The THEMIS array of ground-based observatories for the study of auroral substorms. *Space Science Reviews*, 141(1), 357–387. <https://doi.org/10.1007/s11214-008-9380-x>
- Miyoshi, Y., Matsuda, S., Kurita, S., Nomura, K., Keika, K., Shoji, M., et al. (2019). EMIC waves converted from equatorial noise due to M/Q = 2 ions in the plasmasphere: Observations from Van Allen Probes and Arase. *Geophysical Research Letters*, 46(86), 5662–5669. <https://doi.org/10.1029/2019GL083024>
- Miyoshi, Y., Sakaguchi, K., Shiokawa, K., Evans, D., Albert, J., Connors, M., & Jordanova, V. (2008). Precipitation of radiation belt electrons by EMIC waves, observed from ground and space. *Geophysical Research Letters*, 35(23), L23101. <https://doi.org/10.1029/2008GL035727>
- Nakamura, S., Omura, Y., Shoji, M., Nosé, M., Summers, D., & Angelopoulos, V. (2015). Subpacket structures in EMIC rising tone emissions observed by the THEMIS probes. *Journal of Geophysical Research: Space Physics*, 120(9), 7318–7330. <https://doi.org/10.1002/2014JA020764>
- Ni, B., Cao, X., Zou, Z., Zhou, C., Gu, X., Bortnik, J., et al. (2015). Resonant scattering of outer zone relativistic electrons by multiband EMIC waves and resultant electron loss time scales. *Journal of Geophysical Research: Space Physics*, 120(9), 7357–7373. <https://doi.org/10.1002/2015JA021466>
- Nomura, R., Shiokawa, K., Omura, Y., Ebihara, Y., Miyoshi, Y., Sakaguchi, K., et al. (2016). Pulsating proton aurora caused by rising tone Pc1 waves. *Journal of Geophysical Research: Space Physics*, 121(2), 1608–1618. <https://doi.org/10.1002/2015JA021681>
- Nomura, R., Shiokawa, K., Pilipenko, V., & Shevtsov, B. (2011). Frequency-dependent polarization characteristics of Pc1 geomagnetic pulsations observed by multipoint ground stations at low latitudes. *Journal of Geophysical Research*, 116(A1), A01204. <https://doi.org/10.1029/2010JA015684>
- Obayashi, T. (1965). Hydromagnetic whistlers. *Journal of Geophysical Research*, 70(5), 1069–1078. <https://doi.org/10.1029/JZ070i005p01069>
- Ogawa, Y., Tanaka, Y., Kadokura, A., Hosokawa, K., Ebihara, Y., Motoba, T., et al. (2020). Development of low-cost multi-wavelength imager system for studies of aurora and airglow. *Polar Science*, 23. <https://doi.org/10.1016/j.polar.2019.100501>
- Oguti, T. (1986). Relationships between auroral and concurrent geomagnetic pulsations. *Journal of Geomagnetism and Geoelectricity*, 38(9), 837–859. <https://doi.org/10.5636/jgg.38.837>
- Omura, Y., & Zhao, Q. (2013). Relativistic electron microbursts due to nonlinear pitch angle scattering by EMIC triggered emissions. *Journal of Geophysical Research*, 118(8), 5008–5020. <https://doi.org/10.1002/jgra.50477>

- Ozaki, M., Shiokawa, K., Miyoshi, Y., Kataoka, R., Connors, M., Inoue, T., et al. (2018). Discovery of 1 Hz range modulation of isolated proton aurora at subauroral latitudes. *Geophysical Research Letters*, *45*(3), 1209–1217. <https://doi.org/10.1002/2017GL076486>
- Ozaki, M., Shiokawa, K., Miyoshi, Y., Kataoka, R., Yagitani, S., Inoue, T., et al. (2016). Fast modulations of pulsating proton aurora related to subpacket structures of Pc1 geomagnetic pulsations at subauroral latitudes. *Geophysical Research Letters*, *43*(15), 7859–7866. <https://doi.org/10.1002/2016GL070008>
- Paulson, K. W., Smith, C. W., Lessard, M. R., Engebretson, M. J., Torbert, R. B., & Kletzing, C. A. (2014). In situ observations of Pc1 pearl pulsations by the Van Allen Probes. *Geophysical Research Letters*, *41*(6), 1823–1829. <https://doi.org/10.1002/2013GL059187>
- Paulson, K. W., Smith, C. W., Lessard, M. R., Torbert, R. B., Kletzing, C. A., & Wygant, J. R. (2017). In situ statistical observations of Pc1 pearl pulsations and unstructured EMIC waves by the Van Allen Probes. *Journal of Geophysical Research: Space Physics*, *122*(1), 105–119. <https://doi.org/10.1002/2016JA023160>
- Paxton, L. J., Morrison, D., Zhang, Y., Kil, H., Wolven, B., Ogorzalek, B. S., et al. (2002). Validation of remote sensing products produced by the Special Sensor Ultraviolet Scanning Imager (SSUSI): A far UV-imaging spectrograph on DMSP F-16. *Proc. SPIE 4485, optical spectroscopic techniques, remote sensing, and instrumentation for atmospheric and space research IV*, 4485, 338–348. <https://doi.org/10.1117/12.454268>
- Rodger, C. J., Raita, T., Chilverd, M. A., Seppälä, A., Dietrich, S., Thomson, N. R., & Ulich, T. (2008). Observations of relativistic electron precipitation from the radiation belts driven by EMIC waves. *Geophysical Research Letters*, *35*(16). <https://doi.org/10.1029/2008gl034804>.
- Roldugin, V. C., Roldugin, A. V., & Pilgaev, S. V. (2013). Pc1–2 auroral pulsations. *Journal of Geophysical Research*, *118*(1), 74–81. <https://doi.org/10.1029/2012JA017861>
- Saito, T. (1969). Geomagnetic pulsations. *Space Science Reviews*, *10*(3), 319–412. <https://doi.org/10.1007/BF00203620>
- Sakaguchi, K., Shiokawa, K., Miyoshi, Y., & Connors, M. (2015). Isolated proton auroras and Pc1/EMIC waves at subauroral latitudes. In Y. Zhang, & L. J. Paxton (Eds.), *Auroral dynamics and space weather*. <https://doi.org/10.1002/9781118978719.ch5>
- Selesnick, R. S., Blake, J. B., & Mewaldt, R. A. (2003). Atmospheric losses of radiation belt electrons. *Journal of Geophysical Research*, *108*(A12), 1468. <https://doi.org/10.1029/2003JA010160>
- Semeter, J., & Kamalabadi, F. (2005). Determination of primary electron spectra from incoherent scatter radar measurements of the auroral E region. *Radio Science*, *40*(2), RS2006. <https://doi.org/10.1029/2004RS003042>
- Shiokawa, K., Katoh, Y., Hamaguchi, Y., Yamamoto, Y., Adachi, T., Ozaki, M., et al. (2017). Ground-based instruments of the PWING project to investigate dynamics of the inner magnetosphere at subauroral latitudes as a part of the ERG-ground coordinated observation network. *Earth Planets and Space*, *69*(160). <https://doi.org/10.1186/s40623-017-0745-9>
- Shprits, Y. Y., Kellerman, A., Aseev, N., Drozdov, A. Y., & Michaelis, I. (2017). Multi-MeV electron loss in the heart of the radiation belts. *Geophysical Research Letters*, *44*(3), 1204–1209. <https://doi.org/10.1002/2016GL072258>
- Summers, D., & Thorne, R. M. (2003). Relativistic electron pitch-angle scattering by electromagnetic ion cyclotron waves during geomagnetic storms. *Journal of Geophysical Research*, *108*(A4), 1143. <https://doi.org/10.1029/2002JA009489>
- Troitskaya, V., & Gul'Elmi, A. (1967). Geomagnetic micropulsations and diagnostics of the magnetosphere. *Space Science Reviews*, *7*(5–6), 689–768. <https://doi.org/10.1007/BF00542894>
- Tsyganenko, N. A. (2002a). A model of the near magnetosphere with a dawn-dusk asymmetry: 1. Mathematical structure. *Journal of Geophysical Research*, *107*(A8), 1179. <https://doi.org/10.1029/2001JA000219>
- Tsyganenko, N. A. (2002b). A model of the near magnetosphere with a dawn-dusk asymmetry: 2. Parameterization and fitting to observations. *Journal of Geophysical Research*, *107*(A8), 1176. <https://doi.org/10.1029/2001JA000220>
- Usanova, M. E., Mann, I. R., Kale, Z. C., Rae, I. J., Sydore, R. D., Sandanger, M., et al. (2010). Conjugate ground and multisatellite observations of compression-related EMIC Pc1 waves and associated proton precipitation. *Journal of Geophysical Research*, *115*(A7), A07208. <https://doi.org/10.1029/2009JA014935>
- Yahnin, A. G., Yahnina, T. A., & Frey, H. U. (2007). Subauroral proton spots visualize the Pc1 source. *Journal of Geophysical Research*, *112*(A10), A10223. <https://doi.org/10.1029/2007JA012501>
- Zhang, Y., & Paxton, L. J. (2019). Observations of conjugated ring current auroras at subauroral latitudes. *Journal of Atmospheric and Solar-Terrestrial Physics*, *184*, 1–4. <https://doi.org/10.1016/j.jastp.2019.01.005>
- Zhou, S., Luan, X., Pierrard, V., & Han, D. (2019). Isolated auroral spots observed by DMSP/SSUSI. *Journal of Geophysical Research: Space Physics*, *124*(11), 8416–8426. <https://doi.org/10.1029/2019JA026853>